

***In vivo* activity-dependent plasticity at cortico-striatal connections: Evidence for physiological long-term potentiation**

(basal ganglia/long-term depression/motor learning/striatum/synaptic plasticity)

S. CHARPIER* AND J. M. DENIAU

Institut des Neurosciences, Centre National de la Recherche Scientifique, Unité de Recherche Associée 1488, Université Pierre et Marie Curie, 9, quai Saint-Bernard, F-75005 Paris, France

Communicated by Ann M. Graybiel, Massachusetts Institute of Technology, Cambridge, MA, April 11, 1997 (received for review March 18, 1997)

ABSTRACT The purpose of the present study was to investigate *in vivo* the activity-dependent plasticity of glutamatergic cortico-striatal synapses. Electrical stimuli were applied in the facial motor cortex and intracellular recordings were performed in the ipsilateral striatal projection field of this cortical area. Recorded cells exhibited the typical intrinsic membrane properties of striatal output neurons and were identified morphologically as medium spiny type I neurons. Subthreshold cortical tetanization produced either short-term posttetanic potentiation or short-term depression of cortically-evoked excitatory postsynaptic potentials. When coupled with a postsynaptic depolarization leading the membrane potential to a suprathreshold level, the tetanus induced long-term potentiation (LTP) of cortico-striatal synaptic transmission. Induction of striatal LTP was prevented by intracellular injection of a calcium chelator suggesting that this synaptic plasticity involves an increase of postsynaptic free calcium concentration. Contrasting with previous *in vitro* studies our findings demonstrate that LTP constitutes the normal form of use-dependent plasticity at cortico-striatal synapses. Since excitation of striatal neurons produces a disinhibition of premotor networks, LTP at excitatory striatal inputs should favor the initiation of movements and therefore could be critical for the functions of basal ganglia in motor learning.

Long-lasting changes in synaptic efficacy constitute one of the cellular models for information storage in the brain and behavioral learning (1). Such forms of activity-dependent plasticity classified as long-term potentiation (LTP) and long-term depression (LTD), according to the sign of synaptic modifications, have been found in several regions of the central nervous system. Although the basal ganglia are assumed to be involved in motor learning (2), little information have been obtained about long-lasting synaptic plasticity in this system at least in *in vivo* models.

The cortico-striatal pathway, which provides the main input of the basal ganglia, involves monosynaptic glutamatergic connections (3). *In vivo* (4) and *in vitro* (5, 6) studies have shown that cortically-evoked excitatory postsynaptic potentials (EPSPs) in striatal cells are mainly mediated through α -amino-3-hydroxy-5-methyl-4-isoxazole propionate/kainate receptors and that an *N*-methyl-D-aspartate (NMDA) component becomes significant when synaptic potential reaches a level close to firing threshold (6). In neostriatal slices including the overlying part of the neocortex, it has been shown that high frequency stimulations of the white matter typically induced LTD of cortico-striatal EPSPs (7–10). The induction of LTD in the striatum requires a strong postsynaptic depolarization

(11, 12) but is independent of the activation of the NMDA receptor (8, 11). However, after removing the voltage-dependent block of NMDA receptor channels in magnesium-free medium, the tetanization of cortical fibers produced either short-lasting potentiation (<50 min) (13) or LTP of excitatory synaptic transmission (14). Consequently, it has been recently hypothesized that striatal LTP could occur in pathological conditions such as defective energy metabolism leading to a dramatic calcium influx and subsequent neurodegeneration (9).

Since information about use-dependent cortico-striatal plasticity has been obtained exclusively from *in vitro* preparations, we examined in an intact brain, the ability of cortico-striatal synapses to exhibit long-term changes in their efficacy. We have knowledge of the topographical organization of cortical projections within the striatum (15); therefore, we have been able to test *in vivo* the effects of cortical tetanization on identified cortico-striatal connections.

MATERIALS AND METHODS

Animal Surgery. Experiments were conducted on 18 adult male Sprague–Dawley rats weighing 230–300 g. Animals were initially anesthetized with sodium pentobarbital (66 mg/kg, i.p., Sanofi, Libourne, France) and a cannula was placed in the trachea before they were mounted in a stereotaxic apparatus. Anesthesia was maintained throughout the experiments by additional doses of sodium pentobarbital (6 mg i.p.), administered hourly. In addition, wounds and pressure points were repeatedly infiltrated with lidocaine (xylocaine 2%). Body temperature was maintained between 36 and 37°C with an homeothermic blanket. To obtain stable recordings, rats were immobilized with gallamine triethiodide (Flaxedil, 40 mg i.m., Specia, Paris) and artificially ventilated.

Electrophysiological Procedures. Bipolar steel stimulating electrodes (1-mm tip separation) were inserted in the facial motor cortex (16) at a depth of 1.5 mm from the cortical surface. Intracellular recordings (Fig. 1A), were performed using 2 M K-acetate-filled microelectrodes (40–70 M Ω) in the striatal region related to the stimulated cortical area, at the following stereotaxic coordinates: 9.5 mm anterior to the lambda, 3.5–4 mm lateral to the midline, and 3–5.6 mm ventral to the dura (see ref. 15). In some experiments, the calcium chelator 1,2-bis (2-aminophenoxy) ethane-*N,N,N',N'*-tetraacetic acid (BAPTA, 200 mM) was added to the microelectrode solution. All recordings were obtained using an Axoclamp-2B amplifier (Axon Instruments, Foster City, CA) operated in the bridge mode. Impalements of neurons were considered acceptable when the membrane potential was at

The publication costs of this article were defrayed in part by page charge payment. This article must therefore be hereby marked "advertisement" in accordance with 18 U.S.C. §1734 solely to indicate this fact.

© 1997 by The National Academy of Sciences 0027-8424/97/947036-5\$2.00/0

Abbreviations: BAPTA, 1,2-bis (2-aminophenoxy) ethane-*N,N,N',N'*-tetraacetic acid; EPSP, excitatory postsynaptic potential; LTD, long-term depression; LTP, long-term potentiation; NMDA, *N*-methyl-D-aspartate; *I-V*, current-voltage.

*To whom reprint requests should be addressed.

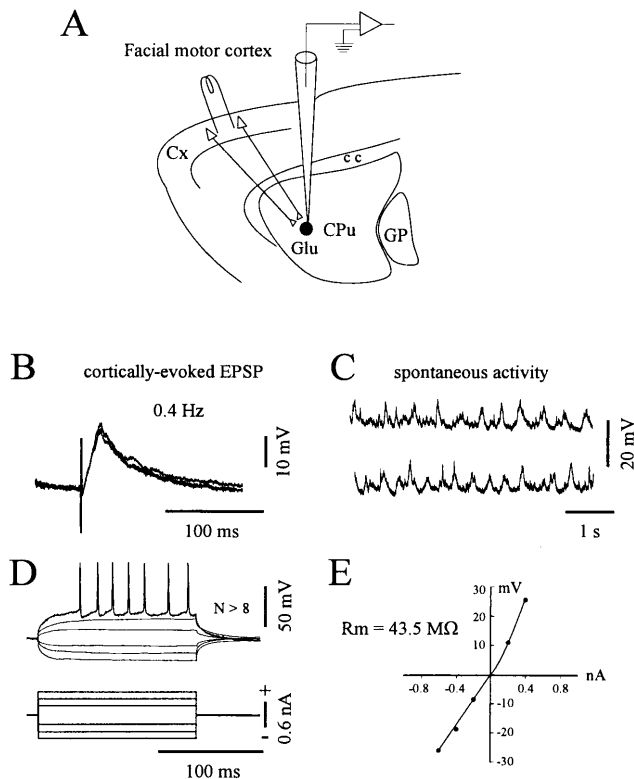


FIG. 1. Scheme of the experimental set-up and electrophysiological properties of recorded neurons. (A) *In vivo* intracellular recordings were obtained from striatal neurons (dark circle) located in the caudate-putamen (CPu) region related to the ipsilateral facial motor cortex. Electrical stimuli applied in this cortical area, through a bipolar stimulating electrode, induce monosynaptic excitation of striatal cells via glutamatergic connections (Glu) (see *Material and Methods* for details). GP, cc, and cx indicate, respectively, the globus pallidus, the corpus callosum, and the cerebral cortex. Data presented in B–E were obtained from the same neuron. (B) Superimposed ($n = 3$) EPSPs elicited by single cortical stimuli delivered at the indicated frequency. (C) Two periods of spontaneous activity showing the presence of regular subthreshold oscillations of large amplitude. In this cell, spontaneous action potentials were not observed at rest (resting membrane potential = -89 mV). (D and E) I - V relationships of striatal neurons. The membrane potential changes (D, upper traces) in response to injection of current pulses (D, lower traces) were measured after averaging. Note the tonic firing triggered by a depolarizing pulse of $+0.6$ nA. The corresponding I - V plot was then constructed (E). The input resistance (R_m) was calculated by the slope of the linear portion of the I - V curve obtained from a series of hyperpolarizing currents. This neuron labeled with biocytin exhibited typical morphological features of spiny type I neurons (not shown).

least -60 mV and the spike amplitude >50 mV. Recordings that did not conform to these criteria were discarded. To measure the input resistance of neurons, current pulses (120- to 250-ms duration, applied at 0.5 Hz) were intracellularly injected through the recording electrode. Test stimulations (200- μ s duration) in the facial motor cortex were applied at 0.4 Hz with an intensity below threshold for action potential induction. Throughout the recording session, cortically evoked EPSPs were averaged ($n = 10$ successive sweeps) and then measured from the baseline to the peak response. In conditioning experiments, cortical tetanic stimulations consisted in short trains (1- to 3-sec duration; applied 2–4 times at 10-sec interval) at 100 Hz. This frequency was chosen since it is usually used to study plasticity at cortico-striatal synapses (7, 8, 10, 11, 14). In all experiments, the intensity of the tetanic stimulation was identical to that used to elicit test EPSPs. Numerical values are given as mean \pm SD. Significant changes in EPSP amplitude were initially assessed by the paired

Student's t test. Because variances differed for some measures, a nonparametric test (Mann–Whitney Rank Sum test) was used to supplement the Student's t test.

Morphological Methods. Labeling of recorded neurons was achieved using microelectrodes (50–80 M Ω) filled with biocytin (1.5%) dissolved in 2 M K-acetate. The dye was injected iontophoretically using positive current pulses (200 ms, 1 nA). After 5–10 min of injection, rats were deeply anesthetized with sodium pentobarbital (200 mg/kg, i.p.) and perfused intracardially with freshly prepared fixative solution (4% paraformaldehyde/0.1% glutaraldehyde in 0.1 M sodium phosphate buffer, pH 7.4). Brains were stored overnight in 10% sucrose solution and cut at 50 μ m on a freezing microtome. After three washes in 0.1 M sodium phosphate buffer (pH 7.4), slices were incubated 12 hr in 1% avidin-biotin complex (ABC Kit Standard, Vector Laboratories) in the presence of 0.5% Triton X-100. After three rinses in phosphate buffer, they were reacted in diaminobenzidine (1%) and cobalt chloride (1%)/nickel ammonium-sulfate (1%)/H₂O₂ (0.01%) solution.

RESULTS

Electrophysiological and Morphological Properties of Recorded Neurons. In a first set of experiments ($n = 10$), intracellular recordings of striatal neurons were performed using K-acetate-filled microelectrodes. The recorded cells were located at various levels within the lateral region of the striatum receiving direct inputs from the facial motor cortex (see Fig. 1A and *Material and Methods*). As classically reported for neostriatal neurons (17), the cells displayed low resting membrane potential (-80.2 ± 6.7 mV, from -71 to -90 mV) and low levels of spontaneous spike discharges. Action potential amplitudes ranged from 58 to 74 mV (65.5 ± 5.9 mV) and their duration (measured from onset to return to baseline) was 1.3 ± 0.16 ms. Electrical stimulations applied in the ipsilateral facial motor cortex evoked short-latency (2.9 ± 1 ms) EPSPs lasting 20–130 ms (Fig. 1B). Increasing the intensity of the stimulation resulted in a progressive enhancement of EPSPs amplitude without change of the latency. The time-to-peak of the cortically evoked EPSPs, measured from the onset of the rising phase, averaged 13.2 ± 2.8 ms. Altogether, these EPSP properties are consistent with the monosynaptic transmission evoked by stimulation of glutamatergic cortico-striatal afferents (5, 6, 17–19). Although most neurons were silent at rest, membrane potential exhibited spontaneous oscillations (Fig. 1C) of large amplitude (5–30 mV). The membrane current-voltage (I - V) relation was determined by measuring the potential deflections in response to injection of series of current pulses (Fig. 1D and E). Input resistance of the cells (32.4 ± 9.7 M Ω) was assessed by the slope of the linear portion of the I - V curve (from -0.2 to -0.8 nA). The intrinsic membrane properties of neurons described here are similar to those previously determined for striatal cells recorded *in vivo* (18, 20) or *in vitro* (11, 13, 17).

To obtain a morphological identification of recorded neurons, in four experiments we combined intracellular recording with injection of biocytin (see *Material and Methods*). In all cases, neurons were located in the striatal projection field of the facial motor cortex. Labeled cells displayed morphological features of the majority class of striatal output neurons, i.e., the type I medium spiny cells (21). Briefly, they exhibited spine-free medium-size somata (diameter between 10 and 20 μ m) and their dendrites were densely covered with spines except on the proximal part.

Effects of Subthreshold Cortical Tetanization Applied at Resting Membrane Potential. Activity-dependent changes in cortico-striatal synaptic efficacy were assessed by measuring the changes in the amplitude of cortically-evoked EPSPs after tetanization of the facial motor cortex. EPSPs were averaged to reduce the effects of natural amplitude fluctuations. In

controls ($n = 6$ neurons), the test stimulation was adjusted to produce subthreshold EPSPs averaging 16.8 ± 2 mV (15–20.4 mV). Neurons had a mean input resistance of 36.8 ± 8.8 M Ω and their resting membrane potential ranged from -73 to -89 mV (-81.2 ± 5.5 mV). Trains of cortical stimulations (see *Material and Methods*) evoked a sustained postsynaptic depolarization of 25 ± 7 mV insufficient to trigger action potentials in the recorded neuron. The membrane potential recovered to its resting level 1–3 seconds after the cessation of the train. We found that in response to this subthreshold tetanization the synaptic transmission could exhibit different forms of short-term plasticity. In two cells, a short-term posttetanic potentiation lasting less than 2 min was observed. The mean EPSP was increased by 24% (Fig. 2A) and 18%, respectively, by the end of the tetanus. In one neuron, where the tetanus-induced depolarization was particularly prominent (+33 mV), the EPSPs amplitude increased gradually to reach 132% of the control value 9 min after trains and this potentiation persisted until the loss of the intracellular recording (18 min after onset of the tetanus). In contrast, a short-lasting (<4 min) depression was observed in two striatal neurons. In the experiment presented in Fig. 2B, the EPSPs amplitude decreased by 76% just after the cortical tetanic stimulations and then rapidly returned to its control level. In the remaining neuron, the tetanic stimulation was without effect on EPSP amplitude. In all cases, the tetanus-induced synaptic changes were not asso-

ciated with modifications in the resting membrane potential or postsynaptic input resistance.

Long-Term Potentiation at Cortico-Striatal Synapses: Role of Membrane Depolarization. To test the effect of membrane polarization on the cortico-striatal plasticity we performed associative experiments where the cortical tetanization was delivered in conjunction with a postsynaptic depolarization. This pairing protocol was applied in 5 neurons having an average input resistance of 25.9 ± 7.9 M Ω and resting membrane potentials ranging from -71 to -90 mV (-79.4 ± 7.9 mV). Prior to the cortical tetanic stimulation, intracellular injection of positive dc current (0.5–1 nA) induced a depolarization of +35 mV (± 23 mV) leading the membrane potential to a suprathreshold level for action potential firing. Using this paradigm, all neurons tested exhibited LTP of EPSP amplitude (Fig. 3). In control condition, the mean EPSP amplitude was 21.3 ± 6.2 mV and during the stable period of LTP this value reached 24.5 ± 6 mV corresponding to a mean increase of

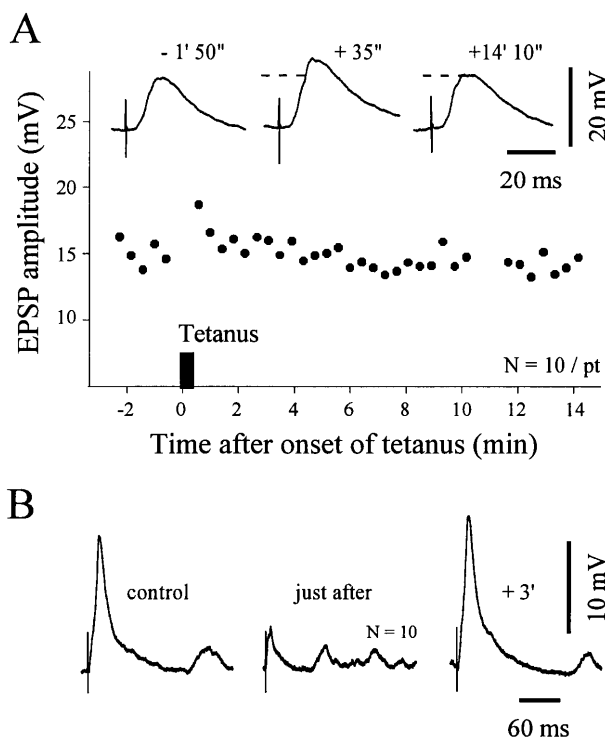


FIG. 2. Effects of subthreshold cortical tetanic stimulation on striatal neurons at resting membrane potential. (A) Example of posttetanic potentiation. The graph shows the time course of the amplitude of striatal EPSPs evoked by single test stimuli applied in the facial motor cortex. ■, The cortical tetanization (train of 1 sec at 100 Hz repeated two times at 10-sec interval, resting membrane potential = -73 mV). The same intensity was used for the test stimulus and the tetanic stimulation. Note that after a short-term posttetanic potentiation, the synaptic efficacy recovered its control level. Traces represent the averaging of 10 successive EPSPs obtained at the indicated times before and after tetanus. The dashed lines indicate the amplitude of the control EPSPs. (B) Example of a short-term depression. Traces represent averaged evoked EPSPs ($n = 10$) obtained at the indicated periods. Parameters of tetanus: train of 2 sec at 100 Hz repeated 4 times at 10-sec interval, resting membrane potential = -85 mV.

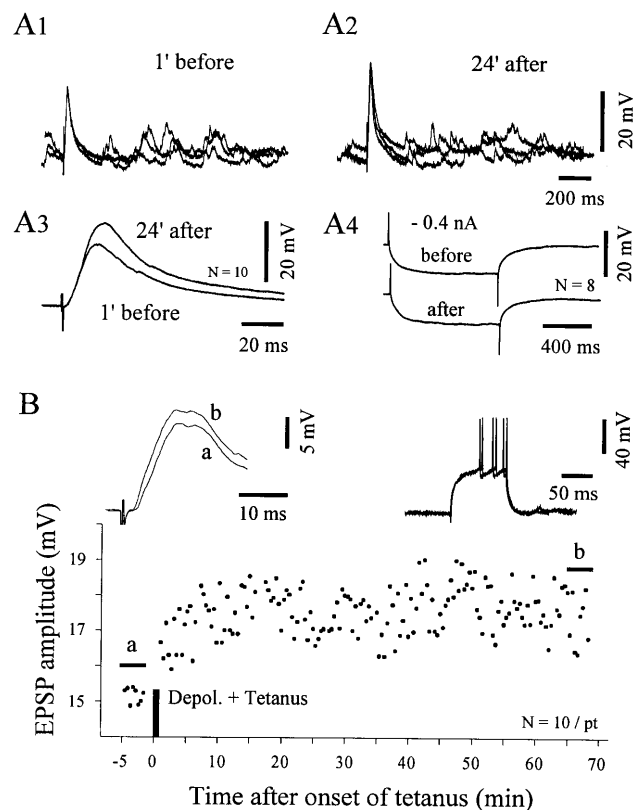


FIG. 3. LTP is induced by cortical tetanic stimulation coupled with postsynaptic depolarization. Results illustrated in A and B are from two separated experiments. (A) Demonstration of striatal LTP. In this experiment, the tetanus was delivered during membrane depolarization induced by an injection of dc current (+0.8 nA) leading the membrane potential from -72 to -37 mV (tetanus parameters: train of 2.5 sec at 100 Hz repeated four times at 10-sec interval). (A1–2) Superimposed EPSPs ($n = 3$) recorded 1 min before (A1) and 24 min after (A2) conditioning. (A3) Superimposition of averaged EPSPs ($n = 10$) showing that the kinetic of synaptic responses was unchanged after potentiation. (A4) The constancy of the mean voltage response to -0.4 nA indicates the input resistance stability of the cell. (B) Time course of striatal LTP. The conditioning protocol consisted in a preliminary depolarization induced by an injection of dc current (+1 nA) followed by tetanic stimulation (train of 1 sec at 100 Hz repeated four times at 10-sec interval). (Inset, Left) Superimposed averaged EPSPs for the periods indicated in the plot below (a, control; b, from +65' to +68' after tetanus) showing that synaptic potentiation was still present more than 1 hr after conditioning ($P < 0.0005$). (Inset, Right) The intrinsic membrane excitability tested by depolarizing current (+0.8 nA) was not modified, as indicated by the superimposed traces obtained just before tetanization and at the end of the recording session.

16.1 ± 8%. In each neuron, the change in EPSP amplitude after conditioning was found to be statistically significant ($P < 0.005$). The maximal increase of the synaptic strength observed in our sample of tested cells was 44%, from 15.8 mV in control condition to 22.8 mV 20 min after tetanus. In one case, the potentiation led a subthreshold EPSP (30.5 mV) to a level sufficient to elicit an action potential in >70% of stimulations. As shown in Fig. 3 A1–A3, striatal LTP was not associated with a change in EPSP kinetics. This observation suggests that the observed potentiation is not due to a development of an additional synaptic conductance. As in preceding experiments (see above), the resting membrane potential and the postsynaptic input resistance (Fig. 3A4) were not modified by the pairing protocols. In all cases, the synaptic potentiation was maintained throughout the posttetanic recording period (>30 min.). In the experiment shown in Fig. 3B, a significant increase of the synaptic efficacy was observed >1 hr after the conditioning. In three cells, LTP was preceded by a short-term (0.5–2 min) posttetanic potentiation. Long-term synaptic depression was never observed in this *in vivo* preparation.

Induction of Striatal LTP: Involvement of Postsynaptic Calcium. Our data suggest that striatal LTP can be obtained *in vivo* when the cortical tetanus is coupled with a postsynaptic depolarization. This was confirmed by the experiment shown in Fig. 4A, in which two successive conditioning protocols were used: (i) a subthreshold tetanic stimulation was applied at resting membrane potential; (ii) the same tetanus was combined with a postsynaptic depolarization (see Fig. 4 legend for details). Although the cortical tetanization applied at rest was without effect on the synaptic strength, a pairing protocol applied in the same neuron induced a sustained increase of the EPSPs amplitude.

The requirement of membrane depolarization in striatal LTP points out a possible involvement of a postsynaptic calcium increase in its induction. To test this hypothesis, we examined the effects of an intracellular injection of the calcium chelator BAPTA on the LTP-induced conditioning. Eight striatal neurons were recorded with BAPTA-filled microelectrode. These cells had a mean resting membrane potential of -78.6 ± 6.4 mV and an input resistance of 32 ± 10.7 M Ω . These values are similar to those obtained with K-acetate-filled microelectrode (see above). In agreement with previous reports (12, 22), calcium chelator injections had no detectable effect on these intrinsic membrane properties. Long-lasting recordings (>60 min.) were obtained from four BAPTA-loaded cells in which a pairing protocol was applied. This latter consisted in a postsynaptic depolarization induced by intracellular current injection ($i_{dc} = +1.4 \pm 0.8$ nA) sufficient to induce tonic firing, followed by the cortical tetanization. Assuming a complete diffusion of the BAPTA into the recorded cells, we used as control responses the evoked EPSPs obtained 15–20 min. after the cell was impaled. The mean amplitude of EPSPs recorded 15 min after tetanus was of $94.8 \pm 6.8\%$ of the control value. As shown in the Fig. 4B, the conditioning could produce a short-term posttetanic potentiation (+13%, $n = 2$) but failed in all cases to induce LTP. These results strongly suggest that LTP in the striatum is caused by a postsynaptic modification and that its induction depends on the level of free calcium.

DISCUSSION

Up to now, knowledge about activity-dependent plasticity at synapses between the cerebral cortex and the neostriatum came exclusively from *in vitro* experiments. From these works, it is assumed that LTD is the “normal” form of long-term plasticity at these connections. However, striatal LTP induction can be obtained *in vitro* under particular pharmacological manipulations such as magnesium-free medium (13, 14) or pulsatile application of dopamine associated with high con-

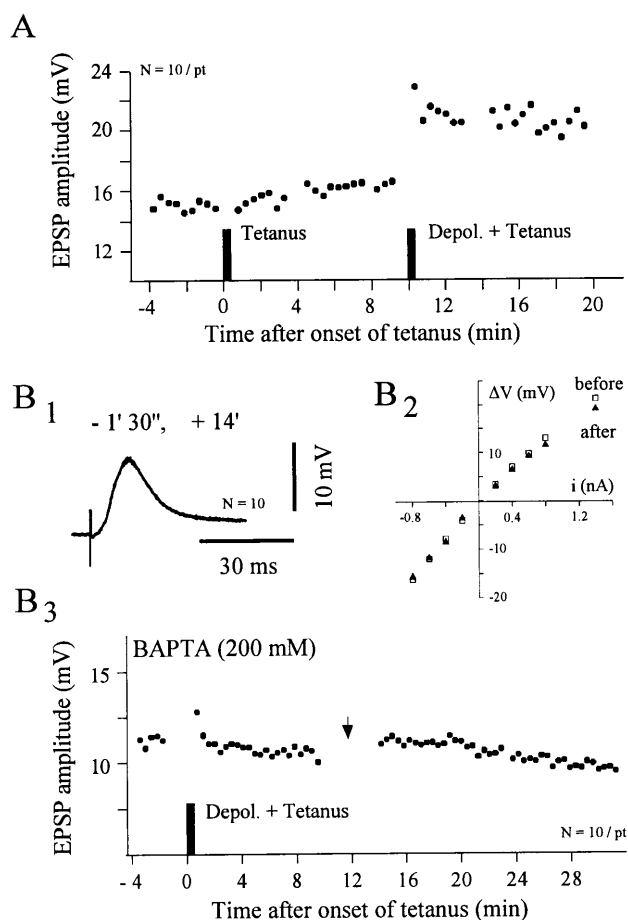


FIG. 4. Involvement of postsynaptic calcium in cortico-striatal LTP. (A) Demonstration that LTP induction needs postsynaptic depolarization. The graph shows the time course of the EPSPs amplitude from a striatal neuron in which two different conditioning protocols were applied. In the first, the cortical trains (100 Hz for 1 sec, repeated three times at 10-sec interval) were applied at rest (resting membrane potential = -81 mV). In the second, the same tetanus was delivered in conjunction with membrane depolarization (from -81 mV to -60 mV; $i_{dc} = +0.7$ nA). Note the rapid and persistent synaptic potentiation induced by the pairing protocol. (B) Induction of striatal LTP is blocked by postsynaptic injection of a calcium chelator. In this experiment where the striatal neuron was injected with BAPTA (200 mM) the tetanic stimulation (100 Hz for 1 sec, repeated three times at 10-sec interval) was associated with membrane depolarization (from -85.7 to -60 mV; $i_{dc} = +2.5$ nA). (B1) Superimposed averaged EPSPs ($n = 10$) recorded at the indicated time after tetanus. (B2) I - V relationship obtained before (\square) and after (\blacktriangle) tetanization showing the input resistance constancy of the recorded striatal cell. Each data point represents the mean value of at least eight successive traces. (B3) After BAPTA injection the pairing protocol caused a short-term posttetanic potentiation immediately followed by the recovery of EPSPs amplitude to control values. (\rightarrow) The recording period used to measure the input resistance of the neuron (see B2).

centration of KCl (10). In fact, our experiments demonstrate that, *in vivo*, the protocols reported to produce cortico-striatal LTD in slice preparations, induce normally LTP but not LTD. It is noteworthy that a similar discrepancy between *in vitro* and *in vivo* preparations has recently been found in the CA1 region of the hippocampus where low frequency (1–5 Hz) stimuli that reliably produce LTD in slice preparations (23) are without effect in anesthetized and awake rats (24).

The *in vivo* striatal LTP described in this report shares common properties with the excitatory LTP described in other brain regions (25). The stable potentiation we observed in the longest experiments lasted >1 hr that is the usual temporal feature to characterize LTP. Moreover, it is induced by

delivering a classical 100-Hz tetanic stimulation to presynaptic inputs and requires suprathreshold postsynaptic depolarization that is normally achieved by synchronization of a large number of converging cortical inputs (26). This is indicative of a basic property of cooperativity that is well established in the hippocampal LTP (27) and suggests that striatal LTP induction needs a coincidental activity in the pre- and postsynaptic elements as predicted by the Hebb's rule for synaptic plasticity (28).

The cellular mechanisms of the *in vivo* cortico-striatal LTP remains unknown. However, the blockade of its induction after injection of the calcium chelator BAPTA in the striatal neurons demonstrates the implication of postsynaptic calcium signaling in the induction process. It is unlikely that the postsynaptic increase of calcium results solely from an activation of voltage-dependent calcium channels since in this case the potentiation decays within 30–40 min. (29). Although a mobilization of calcium from intracellular stores due to activation of striatal metabotropic glutamatergic receptors (30) cannot be excluded, several observations lead to consider that NMDA receptors may play a critical role in striatal LTP. We found that the level of postsynaptic depolarization (-44 ± 18.8 mV) required to induce striatal LTP should reach the threshold level for striatal neurons firing. Recently, it has been clearly demonstrated by Kita (6) that during such depolarization of the striatal cells, the voltage-dependent magnesium-block of NMDA channels is removed and that an NMDA component greatly contribute to cortically-evoked responses. In addition, previous *in vitro* experiments performed in magnesium-free medium have shown that tetanic stimulations of cortical fibers produce a short-term (13) or long-term potentiation (14) of synaptic potentials. Together these results lead to postulate that unmasking of NMDA receptor channels can be achieved *in vivo* by membrane depolarization and consequently could produce, through an inflow of calcium, a classical NMDA-dependent LTP (31).

The present demonstration that cortico-striatal LTP occurs in intact brain provides a new cellular substrate of striatal functions in motor learning. Striatal spiny output neurons are known to integrate information from a large number of cortical neurons (26). Because of their low resting membrane potential and intrinsic membrane properties they require a minimal degree of synchronization in their cortical inputs to be depolarized to the firing threshold (26). In a behavioral context, striatal neurons are assumed to perform a coincidence-detection processing of cortical activities leading to firing discharge and consequently to initiate behavioral output in response to significant sensory events (2). Indeed, it is well established that the striatal discharge produces a GABAergic inhibition of tonically active neurons of the substantia nigra pars reticulata, resulting in a disinhibition of premotor networks in thalamus and brainstem (32). Therefore, it is expected that during learning of a sensory-motor task, LTP may occur at synapses between cortical and striatal cells whose activity became coordinated. In conclusion, we propose that cortico-striatal LTP would favor the acquisition of stimulus-response association through behavioral conditioning (33).

We thank M. J. Besson for encouragements and helpful discussion and J.-C. Behrends for thoughtful comments on the manuscript. We thank also A. Menetrey and P. Nguyen for technical assistance. This work was supported by BIOMED 2 Programme-PL 962215 and the University Pierre & Marie Curie (Paris).

1. Thomson, R. F. (1986) *Science* **233**, 941–947.
2. Graybiel, A. M. (1995) *Curr. Opin. Neurobiol.* **5**, 733–741.
3. Reubi, J. C. & Cuenod, M. (1979) *Brain Res.* **89**, 107–119.
4. Herrling, P. L. (1985) *Neuroscience* **14**, 417–426.
5. Cherubini, E., Herrling, P. L., Lanfumey, L. & Stanzione, P. (1988) *J. Physiol. (London)* **400**, 677–690.
6. Kita, H. (1996) *Neuroscience* **70**, 925–940.
7. Walsh, J. P. (1993) *Brain Res.* **608**, 123–128.
8. Lovinger, D. M., Tyler, E. C. & Merritt, A. (1993) *J. Neurophysiol.* **70**, 1937–1949.
9. Calabresi, P., Pisani, A., Mercuri, N. B. & Bernardi, G. (1996) *Trends Neurosci.* **19**, 19–24.
10. Wickens, J. R., Begg, A. J. & Arbutnot, G. W. (1996) *Neuroscience* **70**, 1–5.
11. Calabresi, P., Maj, R., Pisani, A., Mercuri, N. B. & Bernardi, G. (1992) *J. Neurosci.* **12**, 4224–4233.
12. Calabresi, P., Pisani, A., Mercuri, N. B. & Bernardi, G. (1994) *J. Neurosci.* **14**, 4871–4881.
13. Walsh, J. P. & Dunia, R. (1993) *Neuroscience* **57**, 241–248.
14. Calabresi, P., Pisani, A., Mercuri, N. B. & Bernardi, G. (1992) *Eur. J. Neurosci.* **4**, 929–935.
15. Deniau, J. M., Menetrey, A. & Charpier S. (1996) *Neuroscience* **73**, 761–781.
16. Hall, R. D. & Lindholm, E. P. (1974) *Brain Res.* **66**, 23–38.
17. Jiang, Z.-G. & North, R. A. (1991) *J. Physiol. (London)* **443**, 533–553.
18. Onn, S.-P., Berger, T. W. & Grace, A. A. (1994) *Synapse* **16**, 161–180.
19. Wilson, C. J. (1986) *Brain Res.* **367**, 201–213.
20. Calabresi, P., Mercuri, N. B., Stephani, A & Bernardi, G. (1990) *J. Neurophysiol.* **63**, 651–662.
21. Chang, H. T., Wilson, C. J. & Kitai, S. T. (1982) *J. Comp. Neurol.* **208**, 107–126.
22. Lynch, G., Larson, J., Kelso, S., Barrionuevo, G. & Schottler, F. (1983) *Nature (London)* **305**, 719–721.
23. Mulkey, R. M. & Malenka, R. C. (1992) *Neuron* **9**, 967–975.
24. Errington, M. L., Bliss, T. V. P., Richter-Levin, G., Yenk, K., Doyère, V. & Laroche, S. (1995) *J. Neurophysiol.* **74**, 1793–1799.
25. Bliss, T. V. P. & Collingridge, G. L. (1993) *Nature (London)* **361**, 31–39.
26. Wilson, C. J. (1995) in *Models of Information Processing in the Basal Ganglia*, eds. Houk, J. C., Davies, J. L. & Beiser, D. G. (MIT Press, Cambridge, MA), pp. 29–50.
27. McNaughton, B. L., Douglas, R. M. & Goddard, G. V. (1978) *Brain Res.* **157**, 277–294.
28. Hebb, D. O. (1949) *The Organization of Behavior* (Wiley, New York).
29. Kullmann, D. M., Perkel, D. J., Manabe, T. & Nicoll, R. A. (1992) *Neuron* **9**, 1175–1183.
30. Testa, C. M., Standaert, D. G., Young, A. B. & Penney, J. B. *J. Neurosci.* **14**, 3005–3018.
31. Malenka, R. C. & Nicoll, R. A. (1993) *Trends Neurosci.* **16**, 521–526.
32. Chevalier, G. & Deniau, J. M. (1990) *Trends Neurosci.* **13**, 277–280.
33. Graybiel, A. M. & Kimura, M. (1995) in *Models of Information Processing in the Basal Ganglia*, eds. Houk, J. C., Davies, J. L. & Beiser, D. G. (MIT Press, Cambridge, MA), pp. 103–116.